

Stability Analysis of the 2D linearized unsteady free-surface condition

Lisette M. Sierrevogel and Aad J. Hermans

Department of Applied Mathematics, Delft University of Technology, The Netherlands

Introduction

In recent years, many studies have been carried out to describe unsteady ship motions. These motions are important to predict the seakeeping behaviour of a ship, which includes the interaction between waves and the velocity of the ship. Prins (1995) has developed a two- and three-dimensional time-domain algorithm to compute the behaviour of a cylinder, a sphere and a commercial tanker in current and waves. Since the results were satisfactory, we have extended this method by including a frequency-independent absorbing boundary condition, see Sierrevogel (1996a), and apply it to a LNG carrier at higher speed, see Sierrevogel (1996b).

The increase in the speed causes some numerical instabilities on the free surface. However, the instabilities disappear by using upwind discretization instead of central discretization for the x -derivative. In this abstract, we carry out a theoretical study of the numerical dispersion and damping, and the stability. We follow the work of Raven (1996) and Nakos (1990). The analysis is restricted to the two-dimensional (2D) case for simplicity, while we did also computation in 3D.

1 The time-domain algorithm

In this abstract, we consider the 2D problem we described in Sierrevogel (1996a): A cross-section of a horizontal circular cylinder with radius R , floating in water of infinite depth. A uniform stream flows with velocity U in the positive x -direction and regular waves are travelling in the positive or negative x -direction. The coordinate system is chosen such that the undisturbed free surface coincides with $z = 0$. We consider a potential flow with the velocity potential Φ , satisfying the Laplace equation. By using the dynamic and kinematic conditions and by dividing the potential into a steady ϕ and an unsteady $\bar{\phi}$ part, we get an linearized free-surface condition on the undisturbed free surface. We approximate the unsteady potential $\bar{\phi}$ by the undisturbed flow potential Ux . In Sierrevogel (1996a), we don't do this approximation, but in this analysis it is done for simplicity. Now the linearized free-surface condition becomes

$$\phi_{tt} + g\phi_z + 2U\phi_{xt} + U^2\phi_{xx} = 0 \quad \Rightarrow \quad \phi_z = -\frac{1}{g}\phi_{tt} - \frac{2U}{g}\phi_{xt} - \frac{U^2}{g}\phi_{xx} \quad \text{at } z = 0, \quad (1)$$

To solve the problem, we introduce a Green function, G , satisfying the Laplace equation and we use Green's second theorem. We can use this Green's theorem to calculate the potential on every time step and every panel. Knowing the potential, we are able to calculate the first- and second-order forces and motions. However, in this abstract we are only interested in the stability of the potential on the free surface. Therefore, we are looking at Green's theorem for the potential on the free surface. When both \mathbf{x} and $\boldsymbol{\xi}$ are on the free surface, then $G_\zeta = 0$ and the principal value of the integral along ∂S_{fs} becomes zero. Combining equation (1) and Green's theorem, we get

$$\frac{1}{2}\phi(x, t) - \int_{\partial S_{fs}} \left(\frac{1}{g} \frac{\partial^2}{\partial t^2} + \frac{2U}{g} \frac{\partial^2}{\partial \xi \partial t} + \frac{U^2}{g} \frac{\partial^2}{\partial \xi^2} \right) \phi(\boldsymbol{\xi}, t) G(x - \boldsymbol{\xi}) \, d\xi = RHS \quad \text{at } z, \zeta = 0. \quad (2)$$

with the right hand side, which includes all integrals over the rest of the boundary,

$$RHS = \int_{\partial S \setminus \partial S_{fs}} (\phi G_\zeta - G \phi_\zeta) \, d\Gamma := \int_{\partial S_{fs}} f(\boldsymbol{\xi}) G(\mathbf{x}, \boldsymbol{\xi}) \, d\xi.$$

In practice errors will also be introduced by the discretization of the potential on the hull surface. However, in this abstract we only look at the errors due to the discretization of the free-surface.

2 Continuous Fourier Transform

The Fourier transform of the continuous free-surface equation (2) is derived using the 2D Fourier Transform of the function $\phi(x, t)$ and its inverse are defined by the following pair of equations

$$\tilde{\phi}(k, \omega) = \iint_{-\infty}^{+\infty} \phi(x, t) e^{-i(\omega t - kx)} dx dt \quad \text{and} \quad \phi(x, t) = \frac{1}{(2\pi)^2} \iint_{-\infty}^{+\infty} \tilde{\phi}(k, \omega) e^{i(\omega t - kx)} d\omega dk ,$$

with k the Fourier wave number in the x -direction and with ω the frequency in Fourier space. By using Lighthill's (1959) definition of the Fourier Transform of a log function, we derive the Fourier Transform of the Green function. By using the convolution theorem, we get the Fourier Transform of equation (2). Next we can write continuous Fourier Transform of the potential as follows

$$\tilde{\phi}(k, \omega) = \frac{\tilde{F}(k, \omega) \tilde{G}(k)}{\frac{1}{2} + \left(\frac{\omega^2}{g} - \frac{2U\omega k}{g} + \frac{U^2 k^2}{g} \right) \tilde{G}(k)} .$$

Transforming the solution back to physical space, leads to

$$\phi(x, t) = \frac{1}{4\pi^2} \int_{-\infty}^{+\infty} \int_{-\infty}^{+\infty} \frac{\tilde{F}(k, \omega)}{\tilde{W}(k, \omega)} e^{i(\omega t - kx)} d\omega dk , \quad \text{with} \quad \tilde{W}(k, \omega) = -|k| + \frac{\omega^2}{g} - \frac{2U\omega k}{g} + \frac{U^2 k^2}{g} .$$

with \tilde{W} the continuous spectrum. In section 4, we evaluate the continuous and discrete spectrums, we compare the dispersion relation for the continuous problem with that of the discrete problem. The dispersion relation of the continuous problem is the polar $\tilde{W}(k, \omega) = 0$.

3 Discrete Transformations

In the discrete problem, the solution $\phi(x, z, t)$ is discretized over a free-surface grid of uniform spacing Δx in the x -direction. The collocation point is in the centre of the panel. The solution $\phi(x, z, t)$ is discretized in the time using a uniform time step Δt . To find the discrete form of the free-surface condition, we write equation (2) as follows

$$\frac{1}{2} \phi(x_i, t_n) - \sum_{j=-\infty}^{+\infty} \left(\frac{1}{g} \frac{\partial^2}{\partial t^2} + \frac{2U}{g} \frac{\partial^2}{\partial \xi_j \partial t} + \frac{U^2}{g} \frac{\partial^2}{\partial \xi_j^2} \right) \phi(\xi_j, t_n) \int_{\xi_j - \frac{\Delta x}{2}}^{\xi_j + \frac{\Delta x}{2}} G(x_i - \xi) d\xi = RHS$$

We derive the Fourier Transforms of respectively the integral over the Green function, the x - and t -derivatives, and the free-surface condition, using the 2D Discrete Fourier Transform, and its inverse, which are defined as

$$\hat{\phi}(k, \omega) = \Delta x \Delta t \sum_{m=-\infty}^{+\infty} \sum_{n=-\infty}^{+\infty} \phi(x_m, t_n) e^{-i\theta} \quad \text{and} \quad \phi(x_m, t_n) = \frac{1}{4\pi^2} \int_{-\frac{\pi}{\Delta x}}^{+\frac{\pi}{\Delta x}} \int_{-\frac{\pi}{\Delta t}}^{+\frac{\pi}{\Delta t}} \hat{\phi}(u, s) e^{i\theta} dk d\omega ,$$

where $\theta = \omega n \Delta t - km \Delta x$, and using the discrete convolution theorem. For the first- and second-order x -derivative we use either a central difference scheme or an upwind scheme. By introducing the non-dimensional wave number $\hat{k} = \frac{k \Delta x}{2\pi}$ and frequency $\hat{\omega} = \frac{\omega \Delta t}{2\pi}$, which can be seen as one over the number of step per wavelength or period, the discrete dispersion relation can be written as

$$\begin{aligned} \hat{W} = & -|k| \frac{\pi \hat{k}}{\sin(\hat{k}\pi)} - \frac{\omega^2}{g} \frac{1}{4\pi^2 \hat{\omega}^2} \left(2 - 5e^{-2\pi i \hat{\omega}} + 4e^{-4\pi i \hat{\omega}} - e^{-6\pi i \hat{\omega}} \right) - \\ & \frac{2U\omega k}{g} \frac{1}{16\pi^2 \hat{\omega} \hat{k}} \left(3 - 4e^{-2\pi i \hat{\omega}} + e^{-4\pi i \hat{\omega}} \right) \left(d_1^{(x)} e^{-2\pi i \hat{k}} + d_0^{(x)} + d_{-1}^{(x)} e^{2\pi i \hat{k}} + d_{-2}^{(x)} e^{4\pi i \hat{k}} \right) - \\ & \frac{U^2 k^2}{g} \frac{1}{4\pi^2 \hat{k}^2} \left(d_1^{(xx)} e^{-2\pi i \hat{k}} + d_0^{(xx)} + d_{-1}^{(xx)} e^{2\pi i \hat{k}} + d_{-2}^{(xx)} e^{4\pi i \hat{k}} + d_{-2}^{(xx)} e^{6\pi i \hat{k}} \right) = 0 . \end{aligned} \quad (3)$$

4 Evaluation of the discretization schemes

The evaluation is done first for the zero-speed case, and then the complete dispersion relation, first for waves travelling with the current to the right and then for waves travelling to the left. We compare the the roots of the dispersion relation computed by the continuous and discrete spectrums. We analyse the errors, try to find the wiggles and give some stability criterions. We follow the work of Raven (1996) and Nakos (1990), but our dispersion relation is more complex than theirs. Their continuous and discrete operator, applying linear Kelvin free-surface condition and considering a source contribution, are linear in the wave number. Therefore, the intersection of real part of $Lh(\hat{k})$ with the line $1/Fn_{\Delta}^2$ indicates the wave number of the discretized case and the imaginary part of $Lh(\hat{k})$ is proportional to the numerical damping. In our case we have the analyse the discrete wave number itself

$$k_d = k_c \{1 + C_R(\omega, \Delta\omega, \Delta x) + iC_I(\omega, \Delta\omega, \Delta x)\} . \quad (4)$$

When k_c is negative the wave is travelling to the left and when k_c is positive the wave is travelling to the right. The discrete wave numbers are the roots of the discrete dispersion relation \hat{W} . The term C_R indicates numerical dispersion, an increase ($C_R < 0$) or decrease ($C_R > 0$) of the characteristic length of the associated waves. The term C_I indicates numerical damping ($C_I < 0$) or numerical amplification ($C_I > 0$). Usually one root is nearly the continuous wave number. Any secondary root away from the continuous wave number indicates a spurious wave number. If the imaginary part of this root is positive, wiggles will appear.

In figure 1 and 2, we show the numerical dispersion C_R and damping C_I of the first wave numbers, calculated with equation (3) for downstream waves, as function of \hat{k} . We see that for both discretizations for $\hat{k} < 0.08$ the both the numerical dispersion and damping are small, but there is more numerical damping using the upwind scheme. We also notice that the wave number decreases for $U > .1$ using upwind discretization, while it increases using central discretization.

Using central discretization, the dispersion relation sometimes has two roots for one frequency, see figure 3. The solid lines are the wave number of the continuous dispersion relation. The root far from the continuous wave number has a very large imaginary part, this means that the short waves with that wavelength will amplify rapidly, these numerical instabilities are called wiggles. Figure 3 shows, for instance, that when $\hat{k} = 0.10$ and $U = 0.2$, there are wiggles for $\omega \geq 8$, and no wiggles for $\omega < 8$. In figure 4, we show the critical grid Froude number $Fn_{\Delta x} = U/\sqrt{g\Delta x}$ as function of U . This grid Froude number is used by Nakos (1990) and Raven (1996) in their analysis. In our analysis, we can say that the central discretization is stable that $Fn_{\Delta x} < 0.15$, however it seems that there is still a dependence of the grid size or \hat{k} . More calculations for smaller \hat{k} show the conditions remains $Fn_{\Delta x} < 0.15$.

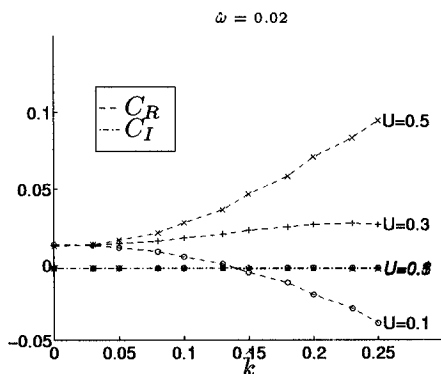


Figure 1: The numerical dispersion C_R and damping C_I for the first root, as in equation (4), as function of \hat{k} , for different speed U , using central discretization

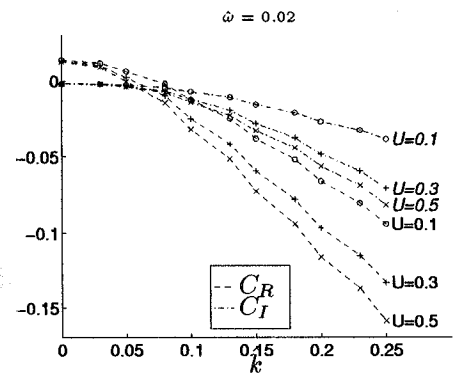


Figure 2: The numerical dispersion C_R and damping C_I for the first root, as in equation (4), as function of \hat{k} , for different speed U , using upwind discretization

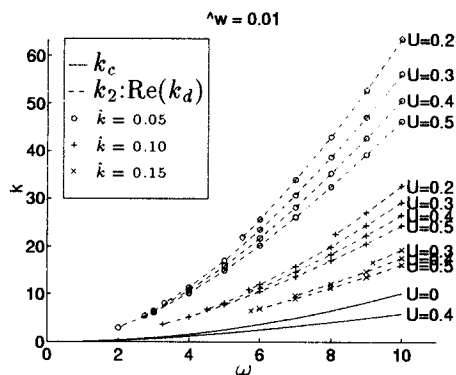


Figure 3: The spurious wave number, as function of the frequency, for different \hat{k} , for $\hat{\omega} = 0.01$ and for different speed U , using central discretization

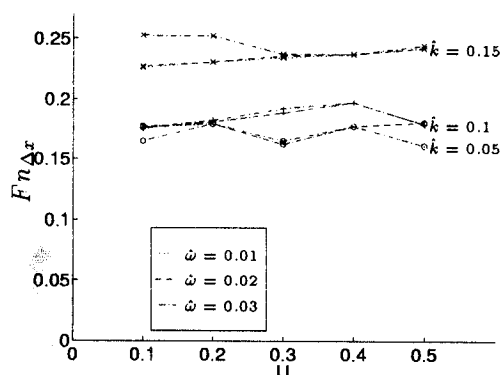


Figure 4: The maximum value of the grid Froude number as function of U , \hat{k} and $\hat{\omega}$, for which the central discretization is stable

5 Conclusions

In this abstract, we developed a theoretical model for a stability analyse of the unsteady 2D linearized free-surface condition. The stability analyse shows us that the numerical method used in Prins(1995) and Siervogel (1996a) is accurate if we use minimum 20 panels per wavelength and 50 time steps per period. We compare central and upwind discretization, and it turns out that downstream with both discretizations the numerical damping and dispersion is less than 1%. The disadvantage of central discretization is the numerical instability which appear when the grid Froude number $Fn_{\Delta x} > .15$. Upstream is the numerical dispersion using upwind discretization larger than using central discretization, but central discretization causes numerical instabilities. Therefore we need more time steps per period.

An other possibility to eliminate the numerical instabilities is a upstream shift of the collocation point, see Raven (1996). A more accurate scheme using less panels can be obtain using higher-order basis functions on the panels, for example quadratic splines, see Nakos (1990). It is possible to evaluate the 3D linearized free-surface condition the same way as we presented in this abstract, only the problem two times three unknowns: $x, \Delta x, y, \Delta y, t, \Delta t$, and therefore complex to evaluate.

In our numerical program we use the double body potential instead of the undisturbed potential flow. We also use a Green's function which satisfies the bottom condition. These points may change the stability condition a little.

References

- Lighthill, M.J. (1959). *Introduction to Fourier analysis and generalised functions*. University Press, Cambridge.
- Nakos, D.E. (1990). *Ship wave patterns and motions by a three dimensional Rankine panel method*. PhD thesis, Massachusetts Institute of Technology, USA.
- Prins, H.J. (1995). *Time-domain calculations of the drift forces and moments*. PhD thesis, Delft University of Technology, The Netherlands.
- Raven, H.C. (1996). *A solution method for the nonlinear ship wave resistance problem*. PhD thesis, Delft University of Technology, The Netherlands.
- Siervogel, L.M. and Hermans, A.J. (1996a). Absorbing boundary condition for floating two-dimensional objects in current and waves. *Journal of engineering mathematics* 30, 573-586.
- Siervogel, L.M. and Hermans, A.J. (1996b). Time-domain calculations of first- and second-order forces on a vessel sailing in waves. *Proc. of the 21st symp. on naval hydrodynamics, Trondheim*.

DISCUSSION

Kim Y.:

- 1) In the unsteady problem, temporal stability is also important. Could you explain your temporal stability criteria?
- 2) Could you show that the limiting case of numerical dispersion when $\Delta x, \Delta t \rightarrow 0$ goes to continuous dispersion relation?

Sierevogel L. + Hermans A.: The authors are grateful to Y. Kim for giving a copy of an unpublished article [1].

- 1) To examine the temporal stability we follow Kim, Kring & Sclavounos [1] and write the discrete dispersion relation as a third-order complex relation

$$\frac{1}{g(\Delta t)^2} Z^3 + \left(\frac{-4}{g(\Delta t)^2} + \frac{-U}{2g\Delta t\Delta x} D^{(x)} \right) Z^2 + \left(\frac{5}{g(\Delta t)^2} + \frac{4U}{2g\Delta t\Delta x} D^{(x)} \right) Z + \frac{\Delta x}{2\hat{G}} + \frac{-2}{g(\Delta t)^2} + \frac{-3U}{2g\Delta t\Delta x} D^{(x)} - \frac{U^2}{g(\Delta x)^2} D^{(xx)} = 0,$$

where $Z = e^{-i\omega\Delta t}$ is the growth factor for each time step. When one of the three roots of this dispersion relation is outside the unit circle in the complex plane, the numerical scheme is temporal unstable. Satisfying the conditions in the paper, the numerical scheme seems to be temporal stable, but this case is too complex to derive a condition analytical, the way Kim, Kring & Sclavounos [1] did.

- 2) The consistency of the discrete dispersion relation can be examined through using Taylor polynomials when $\lim_{\Delta x \rightarrow 0}$ and $\lim_{\Delta t \rightarrow 0}$, then follows

$$\hat{W} = \tilde{W} + O((\Delta x, \Delta t)^2)$$

[1] Kim Y., Kring D.C., & Sclavounos, P.D. (1997). Linear and nonlinear interactions of surface waves with bodies by a three-dimensional Rankine panel method. *Submitted for publication.*